The Astrophysical Journal, 684: L45–L49, 2008 September 1

THREE SUCCESSIVE AND INTERACTING SHOCK WAVES GENERATED BY A SOLAR FLARE

Noriyuki Narukage,[1] Takako T. Ishii,[2] Shin'ichi Nagata,[2] Satoru UeNo,[2] Reizaburo Kitai,[2] Hiroki Kurokawa,[2] Maki Akioka,[3] and Kazunari Shibata[2]

Received 2008 February 16; accepted 2008 July 25; published 2008 August 8

ABSTRACT

We discovered three successive Moreton waves generated by a single solar flare on 2005 August 3. Although this flare was not special in magnitude or configuration, Moreton waves (shock waves) successively occurred three times. Multiple shock waves generated during a single flare have not been reported before. Furthermore, the faster second-generated Moreton wave caught up and merged with the slower first-generated one. This is the first report of shock-shock interaction associated with a solar flare. The shock-plasma interaction was also detected. When the third-generated Moreton wave passed through an erupting filament, the filament was accelerated by the Moreton wave. In this event, filaments also erupted three times. On the basis of this observation, we consider that filament eruption is indispensable to the generation of Moreton waves.

Subject headings: shock waves — Sun: chromosphere — Sun: corona — Sun: flares

1. INTRODUCTION

Solar flares are the largest explosive events in the solar system, and it is easy to imagine that such explosions generate shock waves that propagate in the solar corona. In 1960, a coronal shock wave was indirectly discovered in the Hα spectral line (Moreton 1960; Smith & Harvey 1971); i.e., the intersection of a coronal shock wave and the chromosphere was observed as an Hα wavelike disturbances (Uchida 1968; Uchida et al. 1973). This wave was named a "Moreton wave" after the discoverer. In the 1990s, solar observing satellites were launched and directly detected coronal shock waves in the extreme ultraviolet (Thompson et al. 1998; Biesecker et al. 2002) and soft X-rays (Khan & Aurass 2002; Narukage et al. 2002, 2004; Hudson et al. 2003). Coronal waves have also been directly imaged by ground-based radio observations (White & Thompson 2005; Vršnak et al. 2005). However, observations of shock waves were rare, because the shock wave signatures are much fainter than the flare and propagate very fast. The generation mechanism of a Moreton wave has not been made clear yet.

Here we show the discovery of three successive Moreton waves (shock waves) generated by a single solar flare. Furthermore, we found that the faster second-generated Moreton wave caught up and merged with the slower first-generated one. The merging was also detected in radio as the sudden enhancement of the signal. This is the first report of shock-shock interaction associated with a solar flare. In § 2, we describe the observational data. In § 3, we examine the interaction of shock waves in detail. In § 4, our summary and discussion are presented.

2. OBSERVATIONS

We discovered three successive flare-generated Moreton waves on 2005 August 3 with the Solar Magnetic Activity Research Telescope (SMART) (UeNo et al. 2004) at Hida Observatory of Kyoto University. SMART has the ability to take solar full-disk images in Hα at high spatial resolution (~0.5″, ~360 km on the solar disk). The observing wavelengths are not only Hα center but also ± 0.5 and ± 0.8 Å, thus enabling us to monitor the line-of-sight motion of the chromospheric plasma. It takes about 38 s to obtain one set of these five wavelengths.

A Moreton wave is the chromospheric part compressed and released by a shock wave propagating in the solar corona (Uchida 1968; Uchida et al. 1973). Hence, we need to detect chromospheric downward and upward motion to identify a Moreton wave. SMART can detect such Doppler motion based on observations in Hα $\pm$ 0.5 Å and Hα $\pm$ 0.8 Å in high spatial and temporal resolution. In this event, part of the Moreton wave front was observed in all five wavelengths. However, the three successive Moreton waves were detected in only Hα $\pm$ 0.5 Å, especially Hα $-$ 0.5 Å. In the other wavelengths, it is hard to distinguish between the first and second Moreton waves. The suitable wavelength for the detection of Moreton wave depends on the chromospheric downward and upward motion caused by the coronal shock wave. Because of the observation in various Hα wings, SMART has the advantage of detecting Moreton waves.

A flare started at 04:54 UT near the southeastern limb and generated three successive Moreton waves. Figure 1 (Plate 1) shows the original images in Hα center (Figs. 1*a*, 1*e*, and 1*l*) and "Dopplergrams" (Figs. 1*b*–1*d*, 1*f*–1*k*, and 1*m*–1*s*) observed with SMART. In this Letter, "Dopplergrams" are created using the equation of log ($I_{\rm blue}/I_{\rm red}$), where $I_{\rm red}$ and $I_{\rm blue}$ are the intensity images almost simultaneously observed in the red and blue wings (Hα $\pm$ 0.5 Å), respectively. This method makes the line-of-sight motion clear. In the Dopplergrams, we can identify wavelike disturbances called Moreton waves which successively occurred three times and propagated. The red, green, and blue plus signs indicate the wave fronts of the first, second, and third Moreton waves, respectively. This is the first report of successive Moreton waves. Although there is an observation where Moreton waves propagated both northeastward and southward in the X-class (X10) flare on 2003 October 29 (Liu et al. 2006; Balasubramaniam et al. 2007), these waves were generated at the same time and were not generated successively as in our case. Furthermore, we observed an unprecedented phenomenon: the

[1] Institute of Space and Astronautical Science, Japan Aerospace Exploration Agency, Yoshinodai, Sagamihara, Kanagawa 229-8510, Japan; narukage@solar.isas.jaxa.jp.
[2] Kwasan and Hida Observatories, Kyoto University, Yamashina, Kyoto 607-8471, Japan.
[3] Hiraiso Solar Observatory, National Institute of Information and Communications Technology, Hitachinaka, Ibaraki 311-1202, Japan.

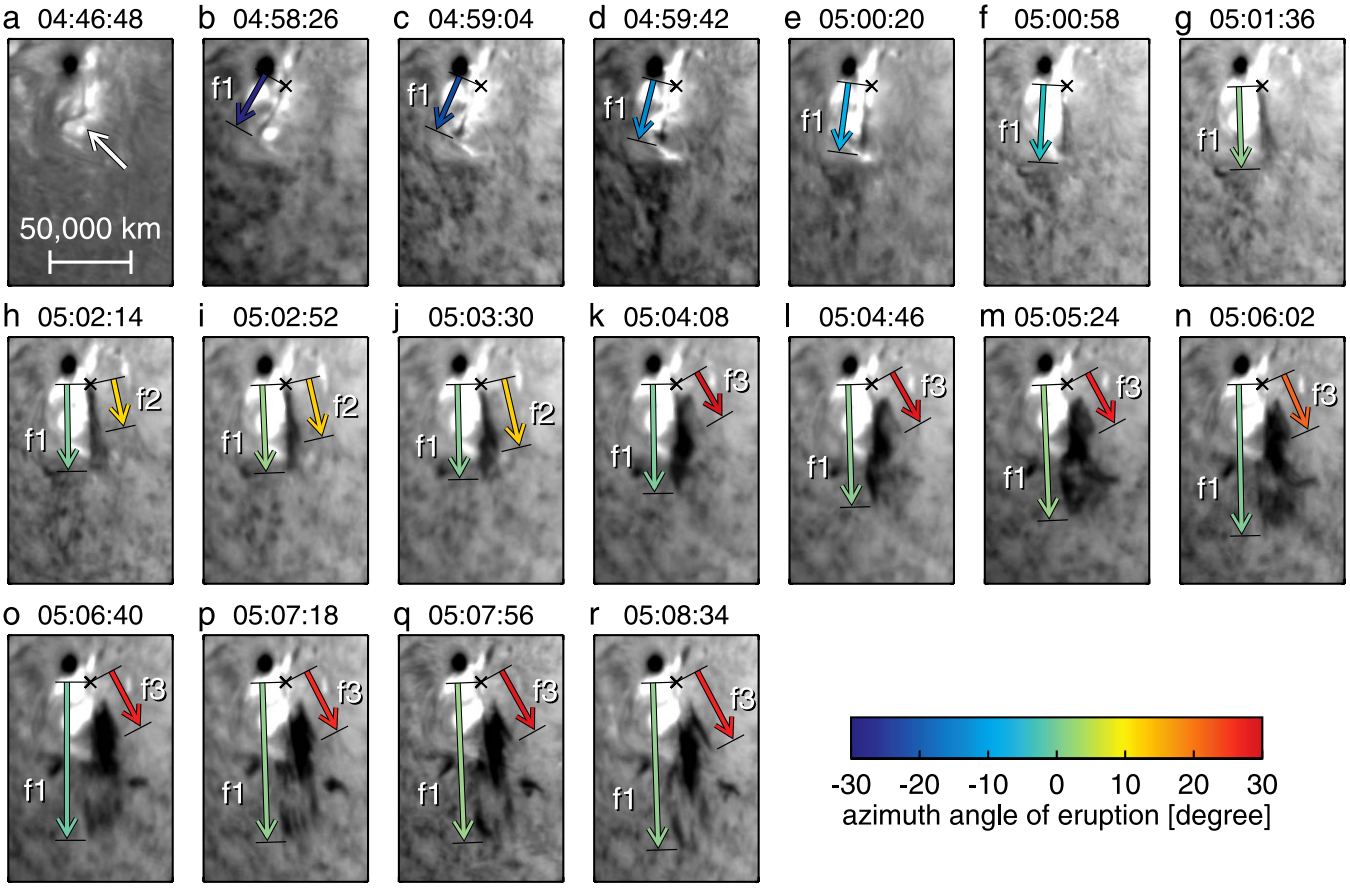

FIG. 2.—Sequential images of erupting filaments. The field of view is shown by the square with dotted line in Fig. 1*t*. (*a*) Preflare stable filament observed in Hα line center. (*b–r*) Three erupting filaments associated with the three successive Moreton waves. These images are created by summing the two images almost simultaneously observed in the Hα blue wings (-0.5 and -0.8 Å) to make erupting (line of sight) motion clear. These three erupting filaments are named "f1," "f2," and "f3" in order of occurrence time. Their footpoints seem to be almost fixed at the same point marked by black crosses. Both ends of the filaments are indicated by black lines. The colored arrows connect such black lines and show the vectors of erupting filaments. The color of arrows indicates the azimuth angle (see color bar), where we define that the southward is 0° of azimuth angle and that the azimuth angle increases counterclockwise.

faster second-generated Moreton wave caught up and merged with the slower first-generated one in 05:01:36–05:02:14.[4]

Figure 2 indicates the motion of filaments. A filament stably existed before the flare as shown in Figure 2*a* observed in Hα line center. Figures 2*b*–2*r* show the series of Hα blue wing images which are created by summing the two images almost simultaneously observed in Hα $-$ 0.5 Å and Hα $-$ 0.8 Å. These images show the moving feature toward us at a line-of-sight speed of several tens km s^{-1}, because the Doppler shifts of Hα $-$ 0.5 Å and Hα $-$ 0.8 Å corresponding to the Doppler speeds of 23 and 37 km s^{-1}, respectively. According to this figure, the filaments erupted three times. These three erupting filaments are named "f1," "f2," and "f3" in order of occurrence time. The relation between the erupting filaments and Moreton waves is described in § 4 in detail.

Figure 3 shows the time evolution of this flare, the Moreton waves, and associated phenomena. Figure 3*a* is the soft X-ray (3–25 keV) intensity, which is emitted from thermal flare plasma with a temperature of 10–20 MK and is roughly a measure of the total released energy by a flare. According to this light curve, this flare was classified as M-class and continued for about 1 hr. The black line in Figure 3*b* is the 2 GHz radio flux observed with the Nobeyama Radio Polarimeters (Nakajima et al. 1985). Gigahertz radio waves are generated by the gyro-synchrotron mechanism of nonthermal electrons. The gray line in Figure 3*b* shows the hard X-ray count rate in 50–100 keV detected by the *Ramaty High Energy Solar Spectroscopic Imager* (*RHESSI*) (Lin et al. 2002). Radio in the GHz range and hard X-rays in 50–100 keV are sensitive to instantaneously released energy. In this flare, three radio flux enhancements were detected around 04:58:30, 05:00:00, and 05:04:15. The hard X-ray count rate was also enhanced in these three timings. We suggest that these energy releases are closely related to the three successive Moreton waves.

3. INTERACTION OF SHOCK WAVES

In this flare, Moreton waves were generated three times and filaments erupted three times. Figure 3*c* shows the position of the Moreton waves with diamonds and erupting filaments with plus signs. Using this figure, we can easily understand the propagation of the Moreton waves. Around 05:01:36, the second Moreton wave (*green diamonds*) caught up with the first wave (*red diamonds*) at a distance of 150,000–200,000 km from the flare site. After this interference, these two waves merged together and continued to propagate. This is the first observation of merging Moreton waves, i.e., shock-shock interaction associated with a solar flare. However, each Moreton

[4] These three successive Moreton waves are easy to identify in movies; see http://www.kwasan.kyoto-u.ac.jp/~naru/three_successive_moreton_wave/index.html.

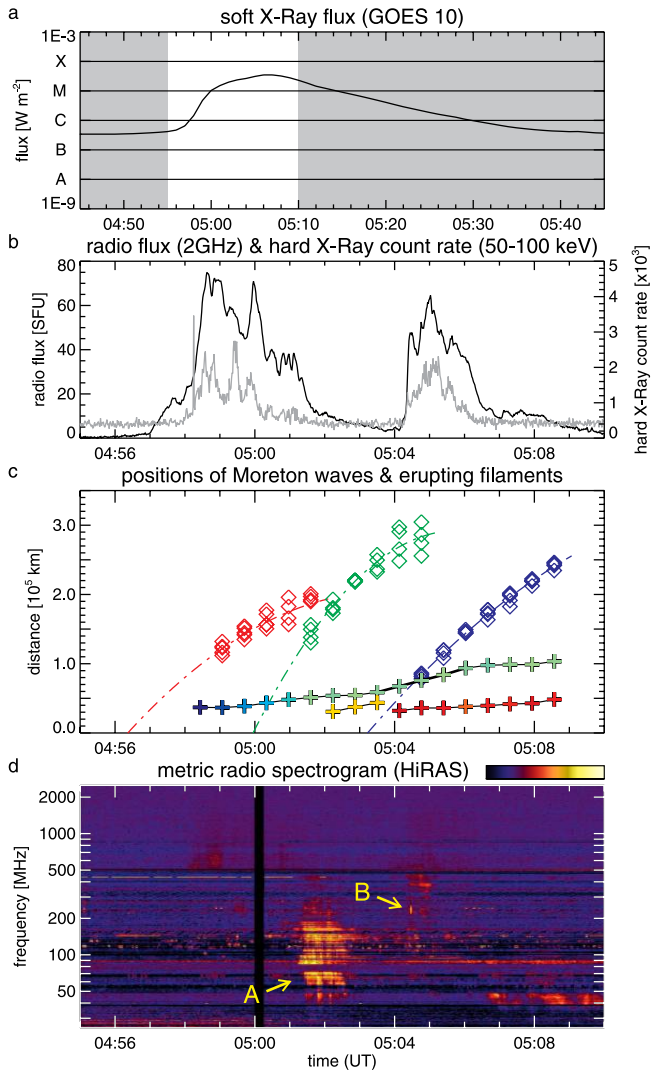

FIG. 3.—Time evolution of the flare, Moreton waves, and associated phenomena. (*a*) Soft X-ray (3–25 keV) intensity observed with the *GOES 10* satellite. The white region shows the period of (*b–d*). (*b*) The black and gray lines show 2 GHz radio flux observed with the Nobeyama Radio Polarimeters and hard X-ray count rate in 50–100 keV detected by *RHESSI*, respectively. (*c*) Propagation of the three successive Moreton waves and eruption of filaments. The red, green, and blue diamonds show the wave fronts of the first, second, and third Moreton waves, respectively. The dash-dotted lines show the second-degree polynomial fits of the wave fronts. We note that we did not apply the polynomial fits to the first Moreton wave front observed at 05:01:36, when the first Moreton wave seems to be interfered with by the second one. The colored plus signs indicate the length of erupting filaments. Their colors mean the azimuth angle as shown in Fig. 2. The blue-green, yellow, and red plus signs are f1, f2, and f3 in Fig. 2, respectively. (*d*) Metric radio spectrogram (25–2500 MHz) observed with the Hiraiso Radio Spectrograph. We note that there are no data from 05:00:00 to 05:00:15 because of the instrument's calibration.

wave itself was not special. The average speeds of the first, second, and third Moreton waves are 460, 740, and 690 km s^{-1}, respectively. The dash-dotted lines in Figure 3*c* show the second-degree polynomial fits. On the basis of these fits, the initial speeds of the Moreton waves are 580, 1200, and 840 km s^{-1}, where initial means the time when each wave front became visible. The decelerations are 1.0, 2.4, and 0.7 km s^{-2}. All three Moreton waves began propagation at a speed of near Alfvén speed (~300–1000 km s^{-1}; see Narukage et al. 2002, 2004) and decelerated during propagation. On the basis of the polynomial fits, the Moreton waves were located several tens of thousands of kilometers away from the flare sites when the energy releases occurred. These properties correspond to previous studies of Moreton waves reported by Warmuth et al. (2004).

Figure 3*d* shows the metric radio spectrogram (25–2500 MHz) observed with the Hiraiso Radio Spectrograph (HiRAS) (Kondo et al. 1995). The excited coronal electrons emit metric radio waves at the fundamental and harmonic plasma frequency of the coronal electrons themselves. This emission is called a radio burst. The drift pattern of the radio burst from high to low frequency means that the site of radio emission moves from the lower to upper corona (Kai 1970). Specifically, a radio burst caused by a shock wave is called a type II burst (Harvey et al. 1974). In this flare, HiRAS detected faint signals drifting from around 500 MHz to low frequency around 04:58:30, 05:00:30, and 05:04:30. These might be type II bursts and related to the Moreton waves. Moreover, the radio signal was suddenly enhanced from 05:01:15 and continued to 05:02:45 as shown by arrow A in Figure 3*d*, just when the second Moreton wave caught up and merged with the first Moreton wave. This drifting pattern consisted of two layers which started from frequencies of 100 and 200 MHz at 05:01:15. The layers of lower and upper frequency were emitted at the fundamental and second plasma frequency harmonics, respectively. On the basis of the coronal electron density model proposed by Newkirk (1961) the radio wave at 100 MHz is emitted by excited coronal electrons at an altitude of 170,000 km. This altitude corresponds to the distance between the flare site and the place where the first and second Moreton waves merged together (150,000–200,000 km; see Fig. 3*c*). Hence, we interpret this radio enhancement to have been caused by the interaction of the shock waves, namely, two shock waves merged together and the power of the merged shock became stronger than the premerged shock waves. Our event is the first report of solar-flare-associated shock-shock interaction.

Gopalswamy et al. (2001) reported a similar phenomenon in interplanetary space. They found merging coronal mass ejections (CMEs) and a related radio enhancement caused by the interaction between shock waves ahead of the first CME and the core of the slow CME, i.e., interaction between a shock wave and a mass of plasma. In our event, not only the shock-shock interaction but also the shock-plasma interaction was detected. When the third Moreton wave (blue diamonds in Fig. 3*c*) passed through the position of first erupting filament f1 (*blue-green plus signs*), the filament was accelerated from 60 km s^{-1} (which is an average speed from 05:01:36 to 05:03:30 in the plane of the sky) to 230 km s^{-1} (05:03:30–05:06:02, which is marked by a black thick line in Fig. 3*c*). We consider that this acceleration of the filament is caused by the third Moreton wave. And, in this timing, the radio signal was enhanced at 250 MHz as shown by arrow B in Figure 3*d*. The 250 MHz radio wave is emitted at an altitude of 8500 km. This value is consistent with the common altitude of filaments. Hence, we argue that this radio enhancement was caused by the interaction between a shock wave and a mass of plasma, like the report of Gopalswamy et al. (2001) and filament oscillations caused by Moreton waves reported in some papers (Eto et al. 2002; Okamoto et al. 2004).

4. SUMMARY AND DISCUSSION

We observed the behavior of shock waves in detail. Although this flare was not special in magnitude or configuration, shock waves successively occurred three times. This means that shock

waves might be generated by a flare more frequently and successively than we had thought based on previous observations. Moreover, these shock waves interacted with each other. This suggests that the configurations of flare-associated shock waves are more complicated than we had thought. These three successive and interacting Moreton waves are unprecedented and thus worthy to report themselves. What is more, these homologous Moreton waves gave us a unique opportunity to understand the generation and propagation mechanism of Moreton waves.

First, we discuss the propagation of Moreton waves. The positions of Moreton waves can be fitted using the second-degree polynomial fits as shown in Figure 3*b*. This suggests that the Moreton waves freely propagated with decelerations. The generation process of Moreton waves, i.e., shock waves, might be completed until the Moreton waves became visible in Hα.

Next, we pay attention to the relation between erupting filaments and Moreton waves. In this event, filaments also erupted three times. The erupting directions of f1, f2, and f3 are southward, south-southwestward, and southwestward, respectively. This shows that the directions of filament eruptions changed counterclockwise in the plane of the sky. This tendency is similar to the Moreton waves. The first Moreton wave began to propagate southward (see Fig. 1*b*), the second wave began to propagate in a direction slightly to the counterclockwise side of the first wave (see Figs. 1*b* and 1*g*), and the third wave in a direction to the counterclockwise side of the second wave (see Figs. 1*g* and 1*m*). We also compared the speed of filament eruptions and Moreton waves. The initial speeds of f1, f2, and f3 were 20, 170, and 50 km s^{-1}, respectively, where the initial speeds were derived using the three initial sequential images for each eruption, namely, Figures 2*b*–2*d* for f1, Figures 2*h*–2*j* for f2, and Figures 2*k*–2*m* for f3. The initial speeds of the Moreton waves are 580, 1200, and 840 km s^{-1}. The second Moreton wave is the fastest, the third is the middle, and the first is the slowest. This is the same order as the speeds of the erupting filaments. Hence, we consider that there are certain correlations between the erupting filaments and Moreton waves in their directions and speeds.

On the basis of the above observational results, we set up a hypothesis that the erupting filaments generated the Moreton waves (shock waves). The initial speeds of the filaments reported in this Letter were 20–170 km s^{-1} in the plane of the sky, and the line-of-sight speeds were about several tens km s^{-1} because the erupting filaments were observed in Hα $\pm$ 0.5 Å and Hα $\pm$ 0.8 Å. These erupting filaments can drive the shock waves (Moreton waves), because Chen et al. (2005) showed that flux rope at a speed of 100 km s^{-1} generates a shock wave in their numerical simulation. If once the filament eruption generated the shock waves, the shock wave propagates faster than the erupting filament. After the shock wave goes away from the erupting filament enough, the shock wave can freely propagate. This is consistent with our observations where the Moreton waves are more than 50,000 km away from the filaments and propagated freely (see Fig. 2*c*). In addition, this hypothesis might explain the gap where the Moreton waves were located several tens of thousands of kilometers away from the flare sites when the energy releases occurred (see Figs. 2*b* and 2*c*). According to Ohyama & Shibata (1997, 2008) not only an X-ray plasma ejection but also an Hα filament started to slowly eject at several tens km s^{-1} about 10 minutes before the impulsive phase, and were suddenly accelerated to several hundreds km s^{-1} just before or at about the onset of the impulsive phase. So, the filament eruptions in our events might also start before the impulsive phase, and might reach at a distance of several tens of thousands km (= several tens km s^{-1} × about 10 minutes) when the flare energy releases were observed in radio and hard X-rays.

As mentioned above, our hypothesis that the erupting filaments generated the Moreton waves (shock waves) is consistent with the observation. However, we have not obtained clear evidence for our hypothesis. To understand the generation and propagation mechanism of Moreton waves, more observations with high temporal and spatial resolution are required. Our results show that new telescopes make it possible to observe the shock waves in detail. In addition to chromospheric observations with SMART, coronal observations with the state-of-the-art X-Ray Telescope (XRT) and Extreme-Ultraviolet Imaging Spectrometer (EIS) on board the *Hinode* satellite will give us more information about flare-associated shock waves (Narukage 2007), e.g., not only plane-of-sky velocity but also line-of-sight velocity, temperature, and density of coronal plasma.

The authors thank especially M. Kadota and all other members of the Kwasan and Hida Observatories for useful comments. We also acknowledge an anonymous referee for his/her useful comments and suggestions. This work was supported by the Grant-in-Aid for the Global COE Program ''The Next Generation of Physics, Spun from Universality and Emergence" from the Ministry of Education, Culture, Sports, Science, and Technology (MEXT) of Japan.

REFERENCES

Balasubramaniam, K. S., Pevtsov, A. A., & Neidig, D. F. 2007, ApJ, 658, 1372
Biesecker, D. A., et al. 2002, ApJ, 569, 1009
Chen, P. F., Fang, C., & Shibata, K. 2005, ApJ, 622, 1202
Eto, S., et al. 2002, PASJ, 54, 481
Gopalswamy, N., et al. 2001, ApJ, 548, L91
Harvey, K. L., Martin, S. F., & Riddle, A. C. 1974, Sol. Phys., 36, 151
Hudson, H. S., et al. 2003, Sol. Phys., 212, 121
Kai, K. 1970, Sol. Phys., 11, 310
Khan, J. I., & Aurass, H. 2002, A&A, 383, 1018
Kondo, T., et al. 1995, Journal of the Communications Research Laboratory, 42, 111
Lin, R. P., et al. 2002, Sol. Phys., 210, 3
Liu, C., et al. 2006, ApJ, 642, 1205
Moreton, G. E. 1960, AJ, 65, 494
Nakajima, H., et al. 1985, PASJ, 37, 163
Narukage, N. 2007, in ASP Conf. Ser. 369, New Solar Physics with the *Solar-B* Mission, ed. K. Shibata et al. (San Francisco: ASP), 205
Narukage, N., et al. 2002, ApJ, 572, L109
———. 2004, PASJ, 56, L5
Newkirk, G., Jr. 1961, ApJ, 133, 983
Ohyama, M., & Shibata, K. 1997, PASJ, 49, 249
———. 2008, PASJ, 60, 85
Okamoto, J. T., et al. 2004, ApJ, 608, 1124
Smith, S. F., & Harvey, K. L. 1971, in Physics of the Solar Corona, ed. C. J. Macris (Dordrecht: Reidel), 156
Thompson, B. J., et al. 1998, Geophys. Res. Lett., 25, 2465
Uchida, Y. 1968, Sol. Phys., 4, 30
Uchida, Y., Altschuler, M. D., & Newkirk, G., Jr. 1973, Sol. Phys., 28, 495
UeNo, S., et al. 2004, Proc. SPIE, 5492, 958
Vršnak, B., et al. 2005, ApJ, 625, L67
Warmuth, A., et al. 2004, A&A, 418, 1101
White, S. M., & Thompson, B. J. 2005, ApJ, 620, L63

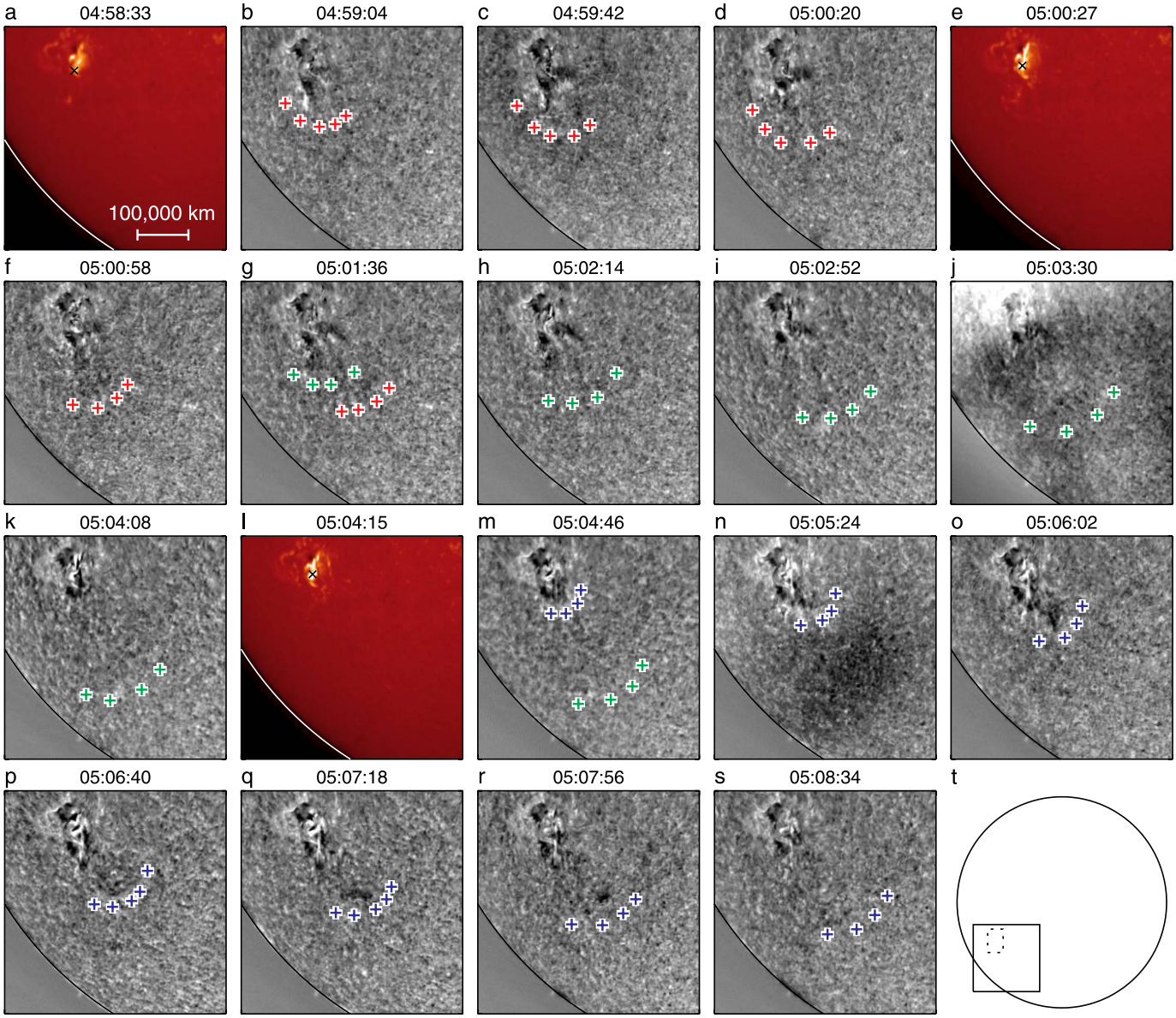

PLATE 1

FIG. 1.—Three successive Moreton waves and associated flare observed with SMART. (*a*, *e*, *l*) Original Hα center images. The black crosses indicate the brightest points in each image, where we suggest that energy was released by the flare and the Moreton waves were generated. (*b–d*, *f–k*, *m–s*) "Dopplergrams" derived by the equation of log ($I_{\rm blue}/I_{\rm red}$), where $I_{\rm red}$ and $I_{\rm blue}$ are the intensity images almost simultaneously observed in the red and blue wings (Hα $\pm$ 0.5 Å), respectively. The red, green, and blue plus signs indicate the wave fronts of the first, second, and third Moreton waves, respectively. (*t*) The square and circle with solid line are the field of view of (*a–s*) and the solar limb, respectively. The square with dotted line indicates the field of view of Fig. 2. We note that the dark configurations located at the center part of (*j*) and the right-bottom part of (*n*) are clouds.